Supplementary Information

High-latitude obliquity as a dominant forcing in the Agulhas current system

Thibaut Caley[1,*], Jung-Hyun Kim[2], Bruno Malaizé[1], Jacques Giraudeau[1], Thomas Laepple[3], Nicolas Caillon[4], Karine Charlier[1], Hélène Rebaubier[4], Linda Rossignol[1], Isla S. Castañeda[2], Stefan Schouten[2] & Jaap S. Sinninghe Damsté[2]

1. Sensitivity of the results on the interpolation method:

Prior to the spectral estimation, the time series are resampled on a regular grid. For the sake of simplicity and because the effects on the frequency spectrum are well known we use linear interpolation to generate time series with a time step of 0.5kyr. This interpolation process acts as lowpass filter and reduces the variance of the signal (e.g. Schulz & Stattegger, 1997) but the effect is limited to frequencies near and higher than the Nyquist frequency (half the original sampling frequency). As we only show and interpret the frequency spectra on orbital timescales (i.e. f>0.06 kyr-1), the interpolation process does not affect any of our results.

To test this statement we repeat the statistical analysis using different time steps from 0.5kyr-5kyr (Figure S3).

When using time steps larger or near the sampling frequency one has to be careful to use all the available data to avoid an increase of aliasing effects. For experiments with timesteps >= 2kyr, we first resample the time series to 0.5kyr resolution using linear interpolation. In the next step we apply a lowpass filter with a cutoff frequency to the final resolution and resample the low-passed filtered time series. In comparison to block averaging, this procedure avoids possible artifacts in the spectral domain caused by the rectangular window (e.g. Priestley, 1981).

The sensitivity of the phase estimates (Table 1) on the interpolation time step (0.5-5kyr) is less than +-0.2kyr and the sensitivity of the coherency estimates is less than +-0.02. The spectral estimates are not sensitive on the interpolation time step in the frequency region of interest (Figure S3).

2. Is the sampling resolution high enough to resolve the precession variability?

The limited sampling resolution of the $U^{K'}_{37}$ and TEX^{H}_{86} (mean timestep 4.5kyr) might reduce the variance at the high frequency side of the spectrum including the precession variability. To estimate the magnitude of this sampling bias, we simulate the sampling process on a prescribed artificial time series. The timeseries consists of an orbital signal (65°N June 21 insolation) superposed on a stochastic background signal (power law spectrum proportional to frequency $^{-2}$, (Pelletier, 1998). Sampling is simulated as point samples (one measurement = one single moment at the measurement) as well as average samples (one measurement = average in the timespan between two measurements) using the time steps of the original proxy time series. The resulting spectra (Figure S4) show that although there is some damping of the precession variability, the sampling resolution is high enough that a presence of a precession signal in the climate signal would be detected. For the case of the Mg/Ca record (mean timestep 2.5kyr) only a very weak damping is expected. Therefore, the finding that Mg/Ca, if analyzed separately (Figure S6) does not show precession variability points to a low or missing precession variability of the climate at the core position.

3. Lateral transport index:

Several early studies have noticed that $U^{K'}_{37}$ SST records are affected by laterally advected allochtonous input. For instance, Benthien and Müller (Benthien and Müller, 2000) showed that core-top $U^{K'}_{37}$ SSTs in the Argentine basin were affected by lateral advection of re-suspended sediments resulting in cold-biased $U^{K'}_{37}$ SST estimates. This lateral transport effect on $U^{K'}_{37}$ SSTs in the Argentine basin has been confirmed by more recent studies (Mollenhauer et al., 2006; Rühlemann and Butzin, 2006). Anomalously warm SSTs during the last glacial period were also observed in a marine sediment core recovered from the South East Indian Ridge (SEIR) at the location of the modern Subantarctic Front and attributed to a strong advection of detrital alkenones produced in warmer surface waters from the Agulhas region to SEIR (Sicre et al., 2005). More recently, Kim et al. (2009) also showed that $U^{K'}_{37}$ indicates much warmer SSTs during the last glacial period compared to all other SST estimates based on diatom and foraminifera assemblages and TEX_{86} in the SEIR. These findings are consistent with core-top TEX_{86} data from the Argentine basin, recording no cold-biased SSTs in contrast to $U^{K'}_{37}$ SSTs (Kim et al., 2008). This is probably due to the rapid degradation of isoprenoid GDGTs compared to that of alkenones (Mollenhauer et al., 2008), which prevents GDGTs from being transported over long (>1000 km) distances. Furthermore, foraminiferal proxies have generally been shown to be least affected by lateral transport (Ohkouchi et al., 2002; Mollenhauer et al., 2008). Taken together, previous studies have shown TEX_{86}, modified now as TEX^{H}_{86}, and Mg/Ca of forams are less sensitive to the lateral transport than $U^{K'}_{37}$. Because core MD96-2048 is located beneath the trajectory where the Agulhas current transports warm Indian Ocean toward the South Atlantic, we suspect a stronger lateral transport of alkenones than GDGTs, thus influencing the $U^{K'}_{37}$ record more than on the TEX^{H}_{86} record. Indeed, another core located southward of our study site and outside of the present Agulhas trajectory (MD96-2077) presents a distinctively different $U^{K'}_{37}$ SST signal (Bard and Rickaby, 2009). Therefore, we calculated SST differences (ΔSST) between $U^{K'}_{37}$ and TEX^{H}_{86} as well as between $U^{K'}_{37}$ and Mg/Ca for MD96-2048, as an indicator of the lateral transport from the Indian Ocean to the South Atlantic (Fig. S8). In general, both ΔSST records show higher values when the relative abundance of ALF (Peeters et al., 2004) decreases implying that lateral fluxes and thus the Agulhas current were stronger when Agulhas leakage was weaker.

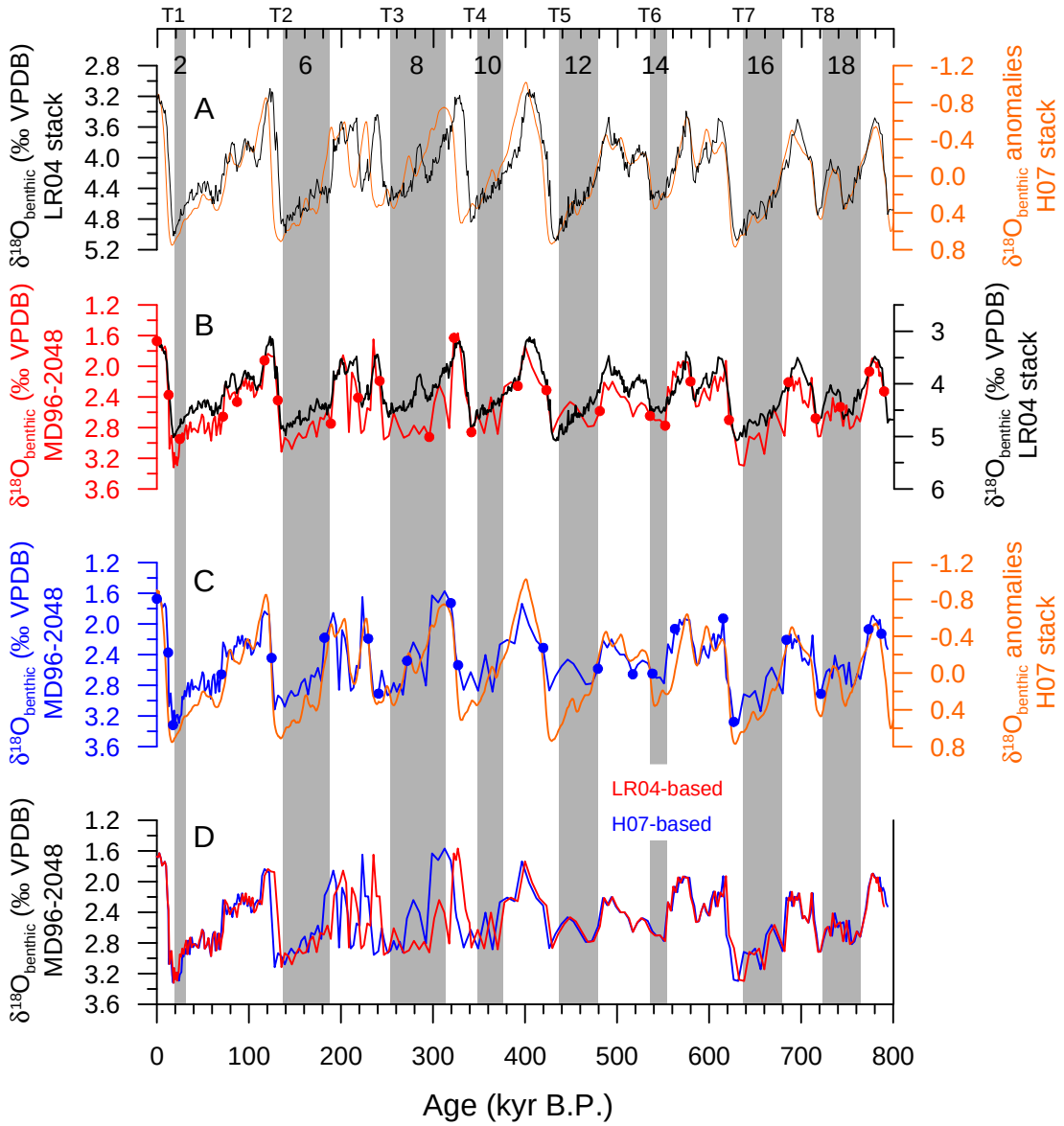

Fig. S1. A) Comparison of original stacks of LR04 (Lisiecki and raymo, 2005; black line) and H07 (Huybers, 2007; orange line). B) The $\delta^{18}O$ of the benthic foraminifer *P. wuellerstorfi* (red line) of core MD96-2048 after age tuning to the LR04 curve (black line) using the Analyseries software (Paillard et al., 1996). C) Similar to (B) but tuned to the H07 curve (orange line). D) Comparison of LR04- (red line) and H07-based (blue line) age models. Filled circles indicate the tie points of MD96-2048 $\delta^{18}O_{benthic}$ values to LR04 (Lisiecki and raymo, 2005; red) and H07 (Huybers, 2007; blue).

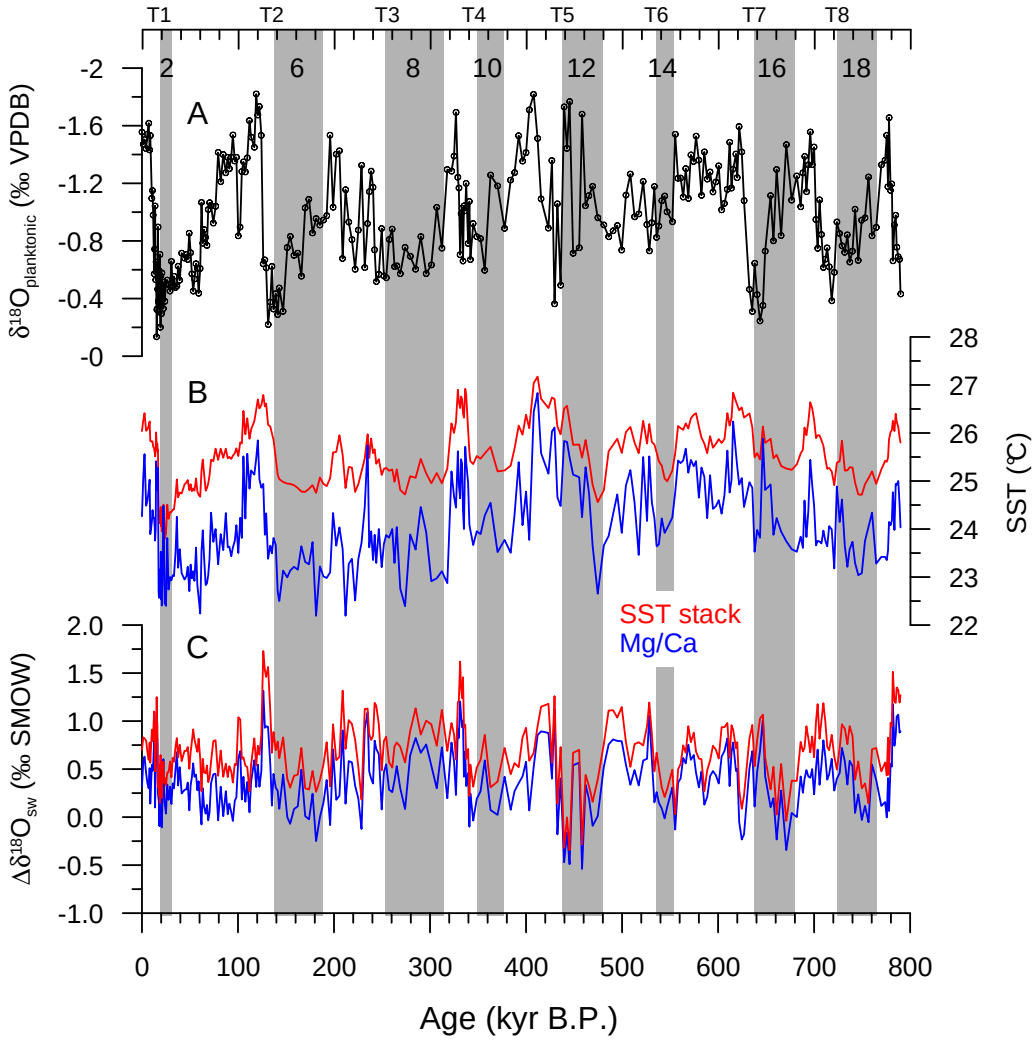

Fig. S2. Sea-surface salinity (SSS, $\Delta\delta^{18}$Osw) reconstruction at core MD96-2048 following the method developed by Duplessy et al. (1991), which leans on the double influence of surface temperature and δ^{18}O isotopic composition of seawater (δ^{18}Osw) on the isotopic values of planktonic foraminifera. A) δ^{18}O measured in shells of the planktonic foraminifer *G. ruber* s. s., B) the SST stack (red line) and Mg/Ca SST (blue line), and C) comparison of SSS reconstructions using the SST stack (red line) and Mg/Ca (blue line) records. We consider that the SST-Mg/Ca approach is, to date, the best tool for the SSS reconstruction because temperature and planktonic δ^{18}O records are based on the same material. However, both curves display the same variations.

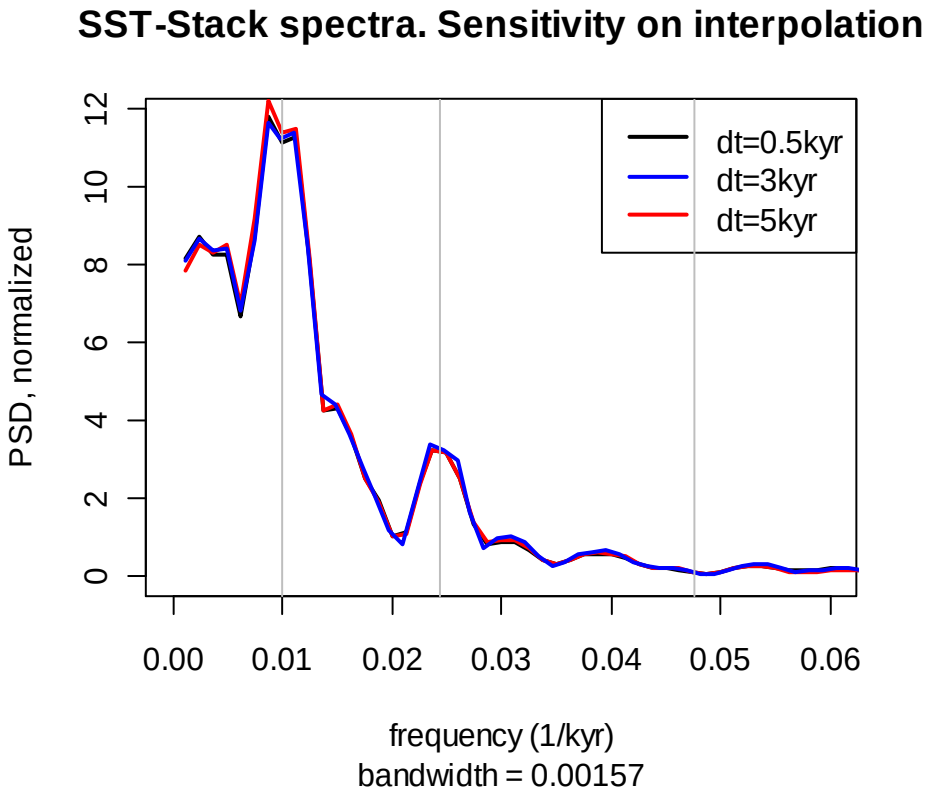

Fig. S3. Sensitivity of the frequency spectra on the interpolation time step. The spectra of the Agulhas SST stack are shown using three different interpolation time steps prior to the spectral calculation.

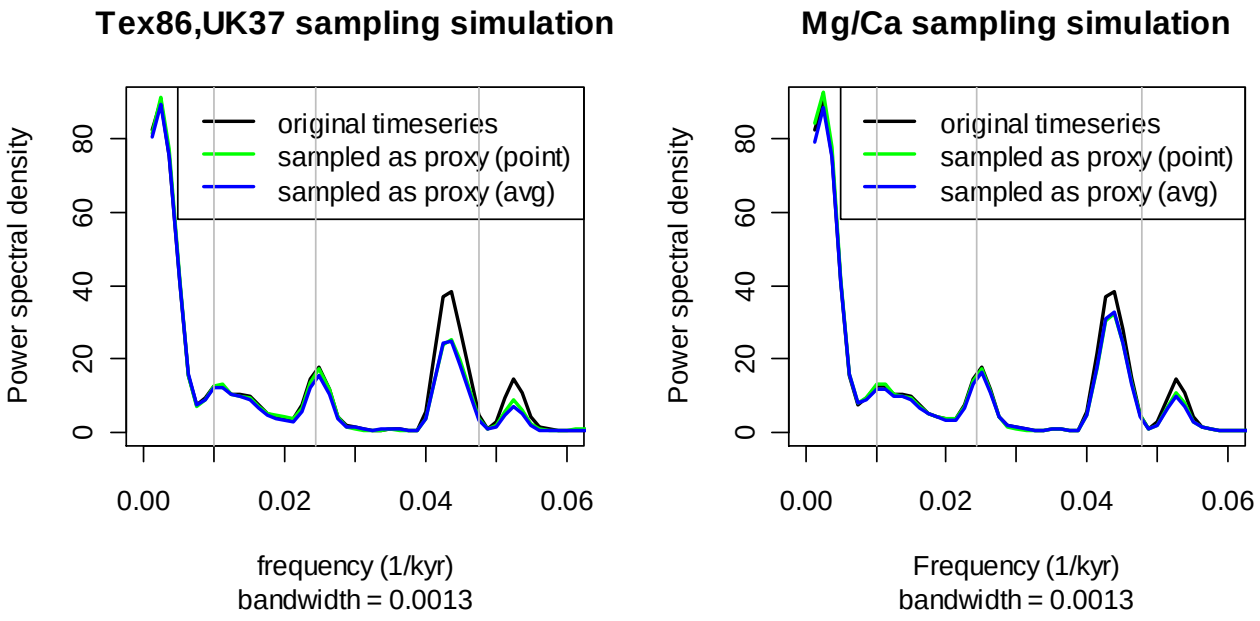

Fig. S4. Effect of the proxy sampling on the reconstructed orbital variability. Frequency spectra of the prescribed time series (65°N summer insolation + stochastic background) (black) and the resampled time series (green and blue), simulating the proxy measurement process. Using the sample time points of Tex86 and Uk37 (mean time step 4.5kyr), the precession amplitude is damped by around 30%. In the Mg/Ca case (mean time step 2.5kyr), most of the precession variability is preserved in the resampled time series.

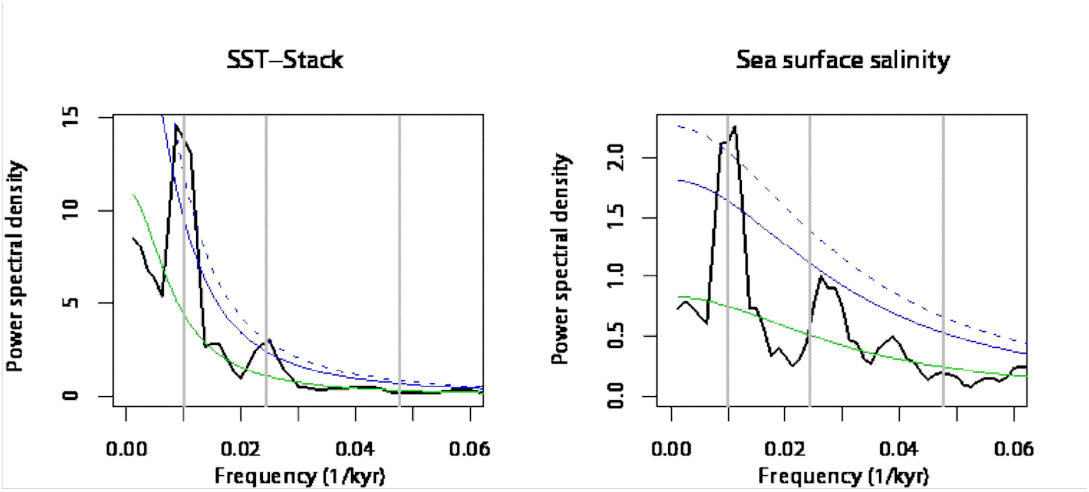

Fig. S5. Power spectrum of SST (top) and $\Delta\delta^{18}O_{SW}$ (bottom) using the alternative Huybers (2007) chronology. The spectrum is estimated using a smoothed periodogram. The spectrum background (green) and 95% (blue continuous) and 99% (blue dashed) confidence intervals are given. The orbital frequencies 1/100 kyr, 1/41 kyr and 1/21 kyr are marked with vertical grey lines.

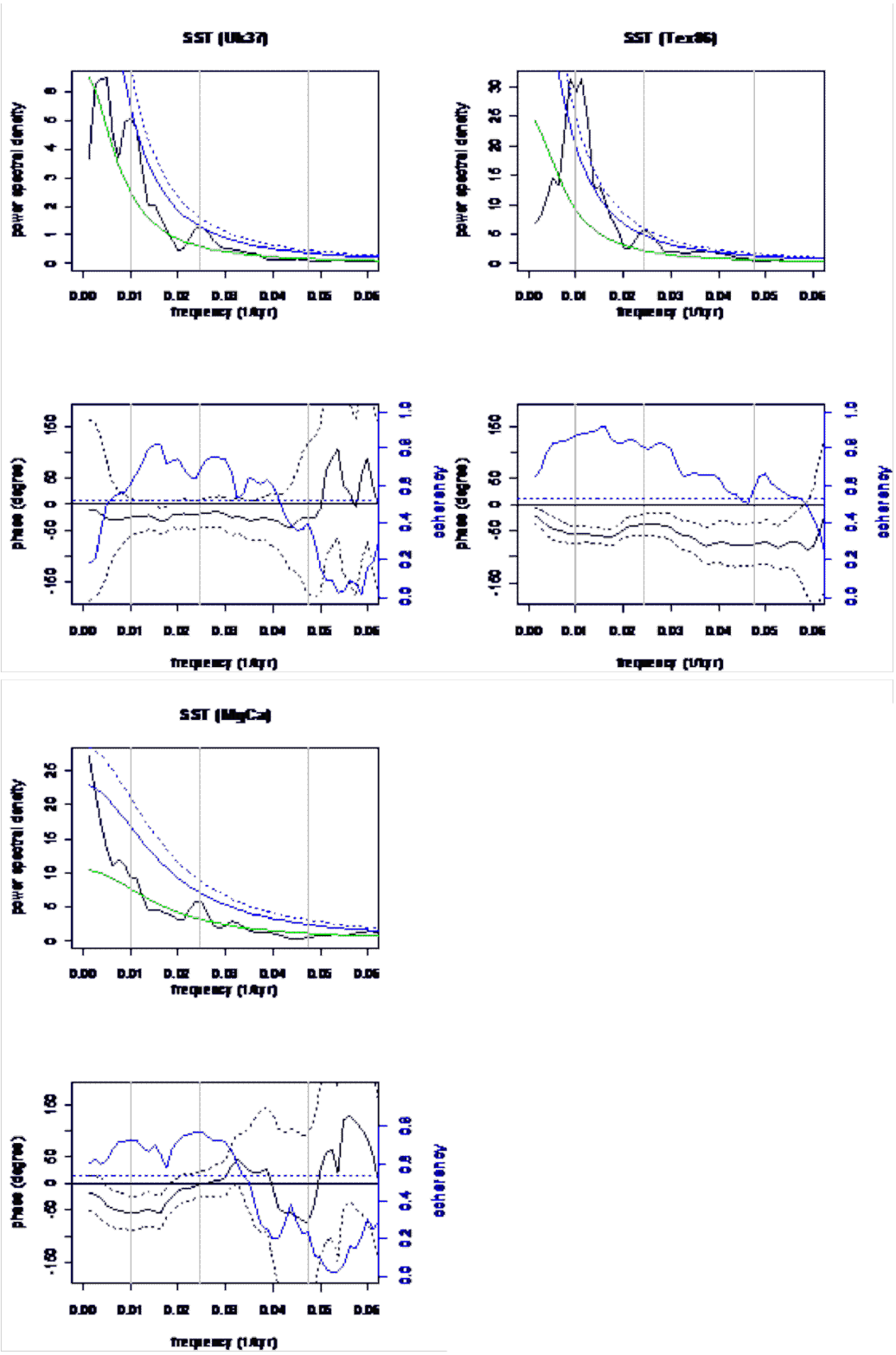

Fig. S6. Frequency spectra for separate Agulhas SST proxies and their coherence and phase relationship relative to global ice volume ($\delta^{18}O_{benthic}$) like Fig. 2. Upper panels: Power spectral density of SST (black line). A red noise background spectrum (green line) and 95% (blue continuous) and 99% (blue dashed line) confidence levels, relative to the red-noise background are given. Lower panels: coherence (blue line) and phase (black line) between the SST proxy and $-1*\delta^{18}O_{benthic}$. The approximate 95% confidence level for the coherence (blue dashed line) and the 95% confidence interval for phase (black dashed line) are given. The orbital frequencies 1/100 kyr, 1/41 kyr and 1/21 kyr are marked with vertical grey lines. Both $U^{K'}_{37}$ and TEX^{H}_{86} show a time lag to $\delta^{18}O_{benthic}$ in the obliquity band. Mg/Ca seems to be in phase with the benthic $\delta^{18}O_{benthic}$.

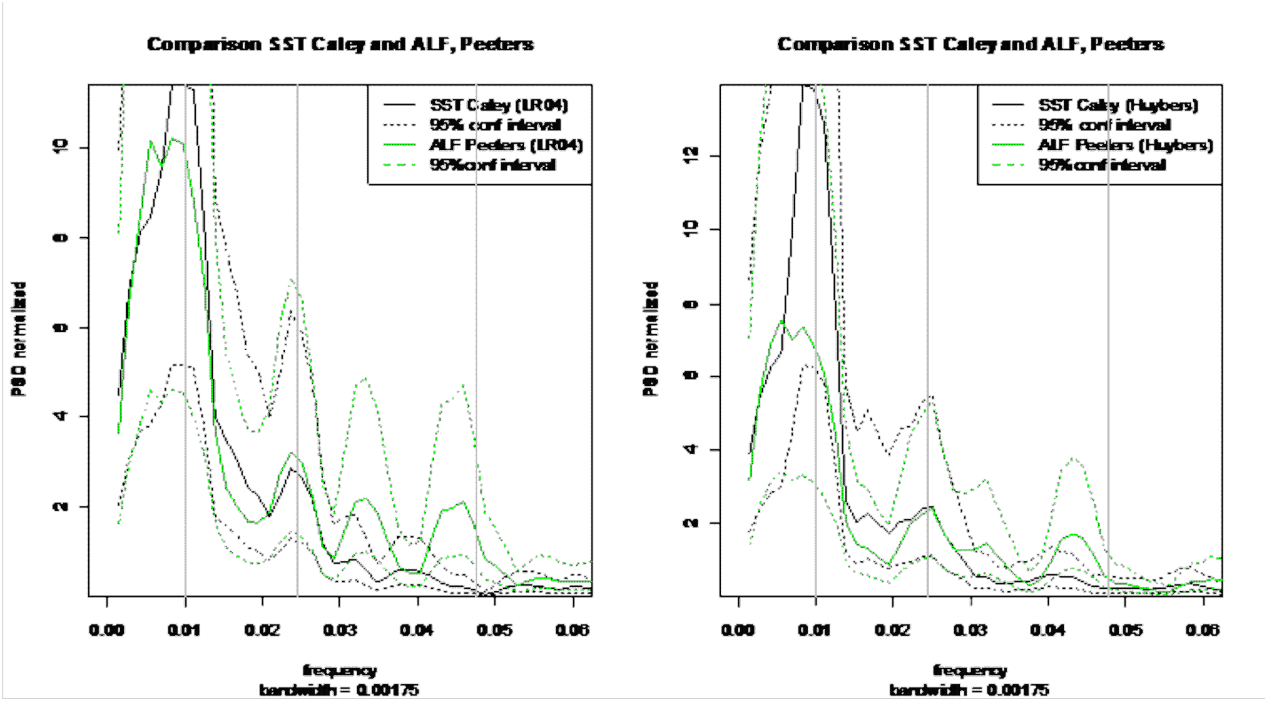

Fig. S7. Power spectrum of the ALF record (Peeters et al., 2004) using the newly established age models in this study.The ALF record is scaled to show the same power in the obliquity band as the SST stack record. The frequency band (1/100, 1/41 and 1/21kyr) are marked with grey vertical lines. One can clearly see that both spectra significantly differ in the precession band. The SST stack record shows no/very weak power in precession band, whereas the ALF record shows similar power as in the obliquity band. We can therefore reject the hypothesis that the presence of the precession band in the ALF record is caused by different tuning techniques.

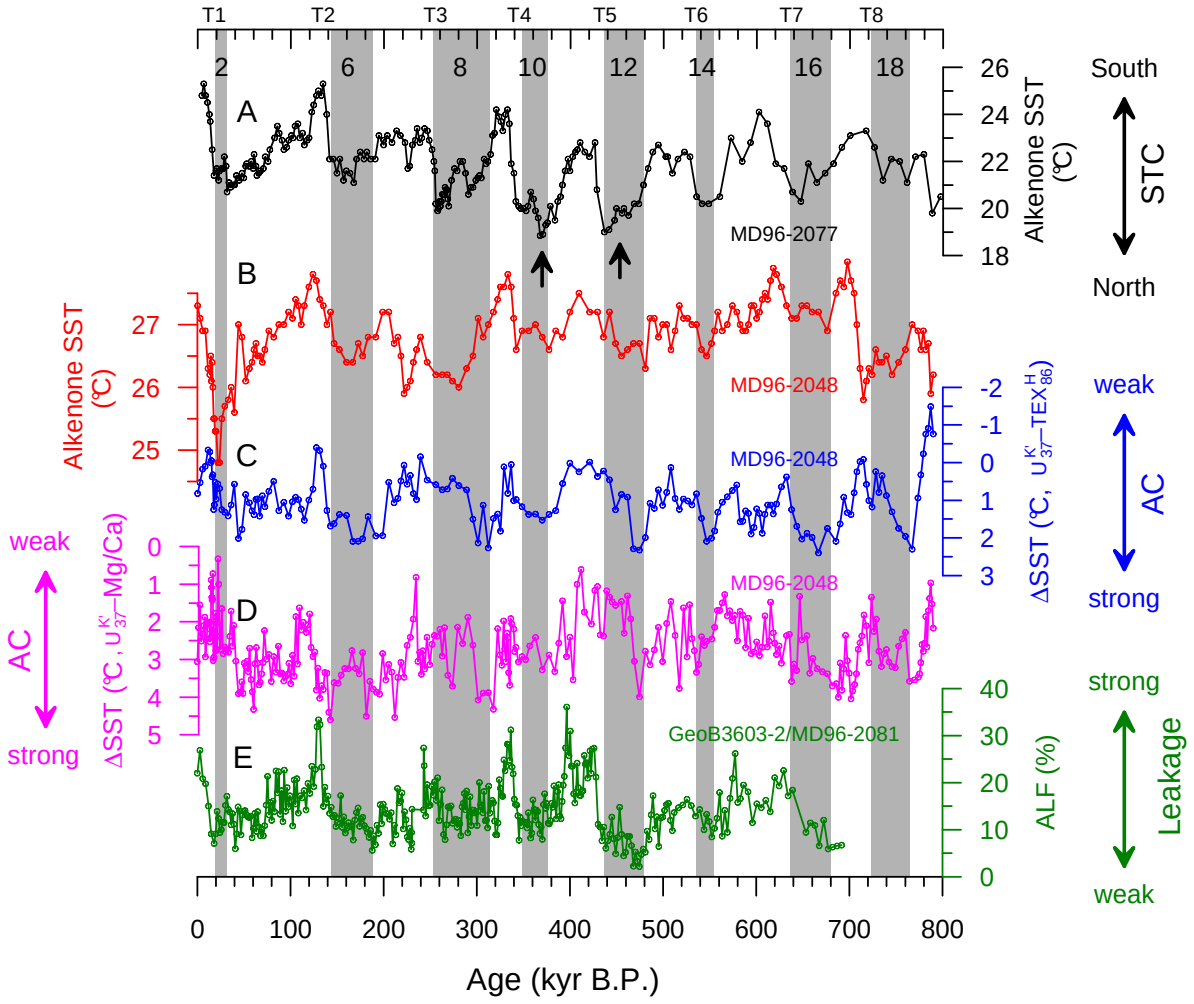

Fig. S8. Relationship between the subtropical convergence (STC) migration and the AC strength and transfer. A) $U^{K'}_{37}$ SST record of MD96-2077, which was used as a proxy of STC migration (Bard and Rickaby, 2009), B) $U^{K'}_{37}$ SST record at site MD96-2048. Warmer glacial SSTs were observed in our record when the STC reached its northern most position (black arrows), C-D) temperature differences (ΔSST) between $U^{K'}_{37}$ and TEX^{H}_{86} and between $U^{K'}_{37}$ and Mg/Ca obtained from MD96-2048 (see Supplementary Information), and E) Agulhas leakage fauna (ALF) record compiled from GeoB3603-2 and MD96-2081, a foraminiferal proxy of the Agulhas leakage (Peeters et al., 2004). Note that a new age model for GeoB3603-2 and MD96-2081 was build based on the correlation between the $\delta^{18}O$ of the benthic foraminifer and the LR04 stack (Lisiecki and Raymo, 2005) to allow comparison with our dataset. AC denotes the Agulhas Current.

Supplementary references

Benthien, A., Müller, P.J.: Anomalously low alkenone temperatures caused by lateral particle and sediment transport in the Malvinas Current region, western Argentine Basin. Deep-Sea Res. I 47, 2369-2393, 2000.

Kim, J.-H. et al. Impact of lateral transport on organic proxies in the Southern Ocean. Quat. Res. 71, 246-250, 2009.

Kim, J.-H., Schouten, S., Hopmans, E.C., Donner, B. & SinningheDamsté, J.S.: Global sediment core-top calibration of the TEX_{86} paleothermometer in the ocean. Geochim. Cosmochim. Acta 72, 1154-1173, 2008.

Mollenhauer, G., Eglinton, T. I., Hopmans, E.C. & Sinninghe Damsté, J.S.: A radiocarbon-based assessment of the preservation characteristics of crenarchaeol and alkenones from continental margin sediments. Org. Geochem. 39, 1039-1045, 2008.

Mollenhauer, G., McManus, J. F., Benthien, A., Müller P. J. & Eglinton, T. I.: Rapid lateral particle transport in the Argentine Basin: molecular ^{14}C and $^{230}Th_{xs}$evidence. Deep-Sea Res. I 53, 1224-1243, 2006.

Ohkouchi, N., Eglinton, T. I., Keigwin, L.D., & Hayes, J.M.: Spatial and temporal offsets between proxy records in a sediment drift. Science 298, 1224-1227, 2002.

Paillard, D, Labeyrie L.D. & Yiou, P.: Macintosh program performs time-series analysis. EOS Trans. AGU 77, 379, 1996.

Pelletier, J.D.: The power spectral density of atmospheric temperature from time scales of 10-2 to 106 yr. Earth and Planetary Science Letters 158(3-4), S.157–164, 1998.

Priestley, M.B.: Spectral analysis and time series. Academic Press, London, 1981.

Rühlemann, C. & Butzin, M.: Alkenone temperature anomalies in the Brazil-Malvinas Confluence area caused by lateral advection of suspented particulate material. Geochem. Geophys. Geosyst. 7, doi:10.1029/2006GC001251, 2006.

Schulz, M., Stattegger, K.: SPECTRUM: Spectral analysis of unevenly spaced paleoclimatic time series. Computers & Geosciences 23, 929-945, 1997.

Sicre, M. A. et al. : Mid-latitude Southern Indian Ocean response to Northern Hemisphere Heinrich events.Earth Plan.Sci. Lett. 240, 724-731, 2005.